Carnosine analogues containing NO-donor substructures: Synthesis, physico-chemical characterization and preliminary pharmacological profile

Carnosine analogues containing NO-donor substructures: synthesis, physico-chemical characterization and preliminary pharmacological profile

Massimo Bertinaria[a], Barbara Rolando[a], Marta Giorgis[a], Gabriele Montanaro[a], Elisabetta Marini[a], Massimo Collino[a], Elisa Benetti[a], Pier Giuseppe Daniele[b], Roberta Fruttero[a,*] Alberto Gasco[a]
[a]*Dipartimento di Scienza e Tecnologia del Farmaco, Università degli Studi di Torino, Via P. Giuria9, I-10125 Torino, Italy*
[b]*Dipartimento di Chimica, Università degli Studi di Torino, Via P. Giuria 7, I-10125 Torino, Italy*

Abstract
The synthesis, physico-chemical, and biological characterisation of a short series of carnosine amides bearing NO-donor nitrooxy functionalities are described. The NO-donor carnosine analogues and their des-NO derivatives display carnosine-like properties, differing from the lead for their high serum stability. The newly-synthesised compounds are able to complex Cu^{2+} ions at physiological pH, displaying significant copper ion sequestering ability, and protect LDL from oxidation catalysed by Cu^{2+} ions. All products show moderately-potent HNE quenching activity. The NO donor compounds **7c-f** relaxed rat aorta strips via a NO-dependent mechanism. In vivo evaluation of organ protection in a model of cerebral ischemia/reperfusion injury, using the selected NO-donor **7e** and its des-NO analogue **7a,** showed that both derivatives protect from hypoxiainduced brain damage, at lower concentrations than carnosine; **7e** also decreased serum TNF-α levels. This class of NO-donor carnosine amides is worthy of further study as potential tools for treating a wide range of chronic vascular and neurodegenerative diseases in which NObioavailability is reduced.

Keywords: Carnosine; Carnosine amides; Cerebral Ischemia; Nitric Oxide; Nitrooxy Derivatives.

1. Introduction
Carnosine **1** is a histidine-containing dipeptide (β-alanyl-L-hystidine) (Chart 1) which in humans is principally present in muscle and nerve tissues [1]. It is rapidly cleaved into its constituents, in both cells and serum, under the action of carnosinases, a group of dipeptidases belonging to the family of metalloproteases [2]. At present, the physiological role of carnosine remains unclear. In vitro, it triggers a variety of biological actions [3]. In particular, it exerts protection against oxidative stress, being a scavenger of reactive oxygen (ROS) and nitrogen (RNS) species, which are responsible for oxidative damage of cellular lipids, enzymes, proteins and DNA [1,4-6]. In addition, carnosine can trap toxic electrophilic α, β- unsaturated aldehydes (e.g., (*E*) 4-hydroxy-*trans*-2,3-nonenal (HNE) and malondialdehyde) deriving from the oxidation of unsaturated membrane lipids [7,8]. It protects proteins from glycation, thus inhibiting the formation of toxic advanced glycation end-products (AGEs) [8-10]. Since oxidative stress and AGEs are involved in the development and progression of some cardiovascular and neurodegenerative diseases [11,12], as well as in ageing, there is currently great interest in carnosine and its derivatives. Recently the effects of carnosine have been extensively studied both in vivo and in vitro in different models of oxidative driven damages, such as neurodegenerative disorders and hypoxia-ischemic injuries [13]. L-carnosine dietary supplementation proved able to promote a strong reduction in the hippocampal intraneuronal Aβ accumulation, and to rescue AD and ageing-related mithocondrial disfunction in 3xTG-AD mice [14]. Unfortunately one limitation in employing L-carnosine as a protective drug is that it is rapidly inactivated by carnosinases. The chemical derivatization of

carnosine is a very promising approach to realize therapeutic carnosinase-resistant molecules based on carnosine. The conjugation of carnosine with several types of organic molecules has the main purpose of reducing the carnosinase action on the peptide moiety, improving the multifunctional activity, because of the potential beneficial role of the conjugating moiety and the synergism with the peptide properties as well.

Different modifications of the carnosine structure have been performed generating a number of multifunctional drug-like molecules which were recently reviewed [15,16]. Recent work on carnosine is directed toward the development of both D- and L-carnosine derivatives stable to carnosinase action. D-carnosine itself proved stable to carnosinase and superior to L-carnosine in some in vitro and in vivo pharmacological models [17,18]. The major drawback with D-carnosine lies in its low bioavailability, since it does not interact with hPEPT1, a transporter responsible for the uptake of a broad array of small peptides in the colon. This problem was addressed with the development of D-carnosine prodrugs; the octyl ester derivative was evaluated in vivo proving able to decrease hypertension, improve dislipidemia and restore renal function in Zucker fa/fa obese rats as well as to inhibit AGEs formation and oxidative stress [19].

Interestingly some new L-carnosine derivatives stable towards carnosinase action were recently synthesized by converting the carboxylic function to an amide and by conjugating the terminal primary amino group to a sugar substructure; these compounds showed carnosinase stability while retaining copper complexing ability [20].

Also our group has recently described some new L-carnosine amides bearing alkyl or arylalkyl substituent at the amide nitrogen endowed with different lipophilicities (chart 1, general structure **I**) [21]. These products share a number of properties with carnosine, including the ability to complex Cu^{2+} ions, to protect LDL from oxidation catalyzed by Cu^{2+}, and HNE quenching activity. Further, in contrast to the lead, they also display high serum stability.

NO is a pivotal signalling messenger in the cardiovascular system. Reduced NO bioavailability and abnormalities in NO-dependent signalling are among the central factors in vascular disease, and loss of endothelium-derived NO is known to be critical in the pathogenesis of vascular diseases, including hypertension, atherosclerosis, and vasospasm with compromised blood flow [22, 23].

Microvascular disorders, occurring with advanced age or in the presence of increased oxidative stress, are consequent on endothelial dysfunction, namely on a reduced capacity of endothelial cells to produce nitric oxide (NO) [24]. Furthermore, chronic mild long-lasting cerebrovascular dysfunction, involving basal NO deficit, significantly contributes to plaque development in Alzheimer's disease (AD) [23]. However, NO's role in the brain is by no means fully elucidated, and both neuroprotective and neurotoxic effects have been widely reported and reviewed [25-27].

As a continuation of our work on NO-donor antioxidant drugs [28], this study aimed to synthesize and characterize new NO-donor carnosine derivatives, with high serum stability. New NO-donor compounds (Chart 1, derivatives **7c-f**) were designed taking into account the relationship between clogD 7.4 and antioxidant activity we previously found (figure 1a); the determination of clogD values for these derivatives (**7c** = -3.12; **7d** = -3.18, **7e** = -3,19, **7f** = -1,72) allowed us to anticipate their optimal hydrophilic-lipophilic balance in order to obtain potent antioxidant molecules. The NO-donor carnosine amides described were obtained by introducing one or two NO donor nitrooxy groups on the lateral chain of the amide nitrogen of scaffolds **7a**,**b**. The introduction of two nitrooxy groups at the ω, ω-1 positions of the propyl chain of **7a** afforded the two diastereoisomers **7d**,**e**.

The preliminary pharmacological profile of these products, its comparison with that of the related des-NO analogues **7a**,**b**, including the results of an in vivo study of the protective effects of **7e** and of **7a** in a model of cerebral ischemia/reperfusion (I/R) injury, are also discussed.

Insert Chart 1

2. Results and discussion

2.1. Chemistry

The NO-donor carnosine amide structures, object of this study, were synthesized by the pathway depicted in Scheme 1. The commercially-available N_{α}-fluorenylmethoxycarbonyl-*N*-trityl-L-histidine (Fmoc-His(Trt)-OH) **2** was coupled with amines **3a**,**b** or with the appropriate NO-donor amines **3c-f,** using the *O*-benzotriazol-1-yl-*N, N, N’ , N’* -tetramethyluronium hexafluorophosphate (HBTU)/1-hydroxybenzotriazole (HOBt)/di-isopropylethylamine (DIPEA) protocol, to give the corresponding intermediate amides **4a-f**. Fmoc deprotection of these intermediates was carried out in DMF at room temperature in the presence of piperidine, to afford the amines **5a-f**. Coupling of free amines with *tert*-butoxycarbonyl protected β-alanine (Boc-β-Ala-OH) in the presence of dicyclohexylcarbodiimide (DCC) afforded **6a-f**, and the subsequent simultaneous Trt/Boc deprotection using 10% (v/v) CF_3COOH in CH_2Cl_2 furnished the target compounds **7a-f**.

Insert Scheme 1

Intermediate substituted benzylamine **3b** was synthesized by alkylation of commercially-available **8,** and the subsequent $LiAlH_4$-mediated reduction of the cyano group. The amines bearing dinitrooxy functionalities **3d**,**e** were synthesized by nitration with fuming nitric acid in CH_2Cl_2 following the method reported elsewhere [29]. Compound **3f** was obtained by reacting tosylate **11** [30] with Boc-protected benzylaminophenol **12** [31] followed by CF_3COOH-mediated deprotection (scheme 2).

Insert Scheme 2

2.2. Stability in human serum

Two isoforms of carnosinase enzyme have been characterized thus far. The first is a cytosolic form (tissue carnosinase) while the second is present in the serum (serum carnosinase). It is not known why the enzyme is present in the serum. Although the neuroprotective effects of carnosine have been widely documented in the literature and recently confirmed by clinical studies in patients with stroke [32], widespread medical use of carnosine is limited by a high rate of its degradation in serum and tissues by carnosinase, which dictates the use of high doses and repeated administration of carnosine. Consequently, an important requisite that analogues of carnosine should posses in order to have therapeutic potential is a good degree of metabolic stability in human serum. For this reason, the NO-donor carnosine amides **7c-f** were studied for their stability in this medium at 37°C. Unlike the lead, which is rapidly metabolized into its constituents following pseudo-first-order kinetics ($t_{1/2}$ = 5 min), all products were stable over 3 h, similarly to the related des-NO amides **7a**,**b**. This is in keeping with the lack of carboxylic group in their structures, which is essential to bind a Zn^{2+} ion present in the active cleft of the enzyme [33].

2.3. Dissociation constants (pK_as) and lipophilicity determination

Dissociation Constants (pK_as) of **7a-f** were determined by potentiometric titration; the results are reported in Table 1. As expected, all NO-donor derivatives and related des-NO analogues show pK_a values that are very close either to that of the basic imidazole centre or of the amino group present on the lateral chain. At physiological pH (7.4) they exist prevalently as

monocharged (92- 93%) and dicharged cations (5-6%). The apparent partition coefficient log $D_{7.4}$ of the products was evaluated by the shake-flask technique, using buffered water (pH 7.4)/*n*-octanol as partition pair (Table 2). As expected, the introduction of nitrooxy function(s) on des-NO amide scaffolds slightly increases the lipophilicity.

2.4. Copper complexes

Particular attention was paid to carnosine's capacity to form complexes with Cu^{2+}, in view of its role in protecting LDL against oxidation induced by Cu^{2+} ions [34,35]. Complex formation between copper (II) and nitrooxy substituted carnosine amides **7c-e** was thus determined, following the same pH-metric technique used to study the parent des-NO analogue **7a**. The study of **7f** and of its des-NO analogue **7b** was hindered by the low water solubility of the products in the experimental conditions. The stability constants of the complexes, expressed as $\beta_{pqr}=[Cu_pL_qH_r]/[Cu]_p[L]_q[H]_r$ for the reaction $pCu + qL + rH = Cu_pL_qH_r$,, where L is the carnosine derivative, and *p, q, r* are the stoichiometric coefficients, the charges being omitted for simplicity.

Since for ligands here studied the dissociation of both peptide and amide hydrogens takes place at too high pH values to allow a reliable evaluation of the relative pK_H in aqueous solution, the concentration [L] in the expression of β_{pqr} takes into account only the hydrogen ion dissociation from protonated imidazole and amino nitrogens. If the presence of metal ion promotes further dissociation of hydrogen ion from peptide and amide group, in the above reaction the species H^+ is subtracted and the index r becomes negative. So the r index is negative if the complex is formed by hydrogen ion dissociation from peptide and/or amide group. From the stability constants reported in Table 1, the ratio between free and total copper (II) concentrations can be calculated, assuming $[Cu]_{total}= 2.5 \times 10^{-6}$ and $[ligand]_{total}= 1 \times 10^{-4}$ M. Analysis of the data shows that the NO-donor carnosine amides display a good ability to sequester copper (II) ions, quite similar to those of the related des-NO analogues, even if their copper(II) complexes are weaker, because of the absence of carboxylate group, than that of carnosine. The capacities of the two diastereoisomers **7d**,**e** to sequester Cu^{2+} ions are similar.

2.5. Biological activity

2.5.1. Antioxidant activity

Free transition-metal ions, especially iron and copper, play important roles in LDL peroxidation. In particular, copper ions at μM concentrations induce generation of free radicals at the low-density lipoprotein (LDL) surface, with consequent oxidative modifications that are of paramount importance in the pathogenesis of a number of cardiovascular and neurodegenerative diseases [36- 39]. This oxidation can be prevented by using copper chelators, such as carnosine and related products. In previous research we assayed the ability of carnosine amides to control this oxidation, by evaluating Δlag time (Δt_{lag}), namely the duration of the period prior to the onset of rapid peroxidation (propagation phase) compared to controls, and the propagation rate of the oxidation (*R*). Δt_{lag} values were found to be dependent on the lipophilicity of the products, the most hydrophilic compounds being the most active (Figure 1b) [21]. Δlag time and *R* values of **7c**-**f**, evaluated under the same conditions used previously, are collected in Table 2. Δlag time values are slightly higher than those of the related des-NO reference compounds **7a**,**b** and of carnosine, and closely fit the correlation reported in figure 1b, between measured log $D_{7.4}$ and antioxidant activity of carnosine amide derivatives. *R* values are slightly lower than those of the reference compounds, and close to that of carnosine. The propagation rates of oxidation in the presence of the two diastereoisomers **7d**,**e** are the same, but its onset is slightly faster for **7d**.

2.5.2. Vasodilator properties

The ability of the target products to supply exogenous NO to blood vessels was evaluated by assessing their capacity to induce relaxation of endothelium-denuded rat-aorta strips, pre-contracted with phenylephrine. All products were capable of relaxing the contracted tissue in a concentrationdependent manner. The vasodilator potencies of the products, expressed as EC_{50} values, are reported in Table 2. They rank in order **7f**>**7e**>**7d**>>**7c**. The vasorelaxant effect was cGMP-dependent, being blocked if experiments were carried out in the presence of 1*H*-[1,2,4]oxadiazolo[4,3-*a*]quinoxalin- 1-one (ODQ), a well-known inhibitor of soluble guanylate cyclase (sGC). Interestingly, **7e** is a vasodilator about three times more potent than its diastereoisomer **7d,** indicating a possible role for the stereoisomery in the interaction of these compounds with the enzyme responsible for their NO production.

2.5.3. HNE quenching activity

As mentioned above, HNE is a particularly abundant reactive aldehyde, generated during lipidic peroxidation through β-cleavage of hydroperoxide derivatives of ω-6 polyunsaturated fatty acids. It is a potent bifunctional electrophile (Michael system and carbonyl group) able to interact with the nucleophile centres of DNA and proteins. After the first electrophile centre has reacted, the second centre undergoes further reaction, producing cross-linking of macromolecules. Carnosine is an efficient quencher of HNE, as well as of its amide derivatives. In order to evaluate the HNE trapping ability of products **7a**-**f**, they were incubated in phosphate buffer, pH 7.4, with the aldehyde at 37 °C. HNE consumption over time was monitored by RP-HPLC [7]. The results obtained after 24 h are summarized in Table 2. The quenching effects on HNE fell in the range 67.2-81.0%, the value for carnosine being 88.8 %. Among the two diastereoisomers, **7e** is a slightly stronger quencher than **7d**.

2.5.4. Cerebral ischemia-reperfusion injury

Reduced blood supply to an organ induces organ injury, whose severity depends on the degree and duration of blood-flow reduction. Reperfusion of ischemic tissue results in further injury. The molecular mechanisms which underlie I/R injury are complex and not fully understood.
It is certain that overproduction of reactive oxygen metabolites during reperfusion, in particular of the superoxide anion ($O_2^{\cdot -}$), plays a central role. Hydrogen peroxide (H_2O_2) is formed from this radical by action of superoxide dismutase (SOD). H_2O_2 is a source, through the Haber-Weiss reaction, of the highly-toxic hydroxyl radical ($OH^{\cdot}$), the principal agent responsible for the cell damage induced by oxidative stress. Release of pro-inflammatory cytokines, increased expression of endothelial adhesion molecules and of chemotactic factors, as well as infiltration of leukocytes, also play important roles in post-ischemic inflammation, contributing to progression of tissue damage [40]. Several studies have clearly demonstrated that carnosine exerts beneficial effects against I/R-induced organ damage, including the brain [41-43]. However, its rapid and complete enzymatic hydrolysis by carnosinases severely limits its potential therapeutic use. The role of NO in I/R is complex. It exerts either protective or toxic effects, depending on the level, location, source, and environment [44,45]. Beneficial effects in I/R are due to its numerous capabilities: it relaxes vascular smooth muscle, protects the microvasculature, prevents neutrophile infiltration, maintains vascular permeability, modulates cytokine expression, as well as displaying antioxidant, anti platelet-activating factor, and antimicrobial properties. Consequently, a supply of exogenous NO (NO-donors) might have beneficial effects in acute ischemic damage [46,47]. In order to reinforce experimental evidence of the therapeutic potential of the NO-donor carnosine amides described here, the most promising derivative (compound **7e)**, its des-NO analogue **7a**, and carnosine (**1**) were tested in a well-known in vivo model of cerebral I/R injury, as we report

elsewhere [48]. In comparison with brain sections obtained from sham-operated rats, those rats that underwent cerebral I/R injury showed an infarct volume of 31.6 ± 4.1% of the total brain. As shown in Figure 2, compound **1** administration (1 g/kg) almost halved the I/R-induced infarct volume. Our results are consistent with previous studies showing that exogenously administered carnosine evoked a marked reduction in infarct size when administered before the ischemic injury either in adult and neonatal rat models [49-51]. Carnosine has been reported to exert protective effects on neurological symptoms and animal mortality even when injected into the blood stream after the ischemic event [52]. Here for the first time we show that a marked reduction in the mean size of the ischemic area was also measured when two carnosinase-stable derivatives, compound **7e** and its des-NO analogue **7a,** were administered at 500 mg/kg, without any significant difference among groups. These results demonstrate that both of these carnosine derivatives exert protective effects against I/R injury, at lower doses than is required for carnosine, being about four time more active than the lead (**1**). In our acute experimental model, the potential further beneficial effect of NO release by compound **7e** was blunted by the predominant role of antioxidant activity due to the carnosine amide substructure.
This observation is in keeping with previous in vivo and in vitro studies reporting that carnosine neuroprotective effects were almost entirely attributable to its ability to inhibit and/or prevent oxidative and nitrosative stress [13]. However, recently, carnosine has also been demonstrated to reduce glutamate excitotoxicity through the regulation of the glutamate transporter-1 [50], to protect the bioelectric activity of nervous cells by restoring the activity of the glutamatergic and GABAergic receptors [53] and to affect the apoptotic cascade in the ischemic brain by inhibiting mRNA expression of apoptosis-inducing factor and caspase-3 [51]. Here we show that the NO-donor carnosine derivative **7e** may modulate cytokine production in the ischemic brain. In fact, when serum tumor necrosis factor (TNF)-α concentrations were measured, as typical marker of the excessive inflammatory response associated with I/R injury (Figure 3), the two-fold increase in TNF-α levels evoked by I/R was significantly reduced by administering compound **7e**; in contrast, both des-NO analogue **7a** and carnosine had no effect on TNF-α production. TNF-α is one of the key immunomodulatory and pro-inflammatory cytokines, which has been clearly demonstrated to be up-regulated during cerebral I/R injury [54]. Recent evidence also suggests that chronic exposure to high levels of TNF-α may induce changes in both lipid and glucose metabolism, likely to exert pro-atherogenic effects, thus promoting the development of atherosclerotic lesions [55]. Therefore, although decreased cytokine production is not essential for protection against acute cerebral injury, it is possible that the decreased cytokine production evoked by compound **7e** might significantly contribute to the potential protective effects of its prolonged administration in vascular disorders characterized by high levels of chronic inflammation, such as I/R-induced organ damage, atherosclerosis and Alzheimer's disease.

3. Conclusions

In conclusion, we have designed and realized a new series of carnosine amide derivatives with NO-donor properties. The results of this study demonstrate that our compounds are a new class of NO-donor antioxidants endowed with HNE scavenging and Cu^{2+} chelating properties, able to inhibit LDL oxidation. Preliminary pharmacological characterization of **7e** shows that these compounds are worthy of additional study as potential tools in the treatment of complex vascular and neurodegenerative disorders, whose onset and progression involve oxidative stress and decreased NO availability.

4. Experimental

4.1. Instrumentation and chemicals

Determination of melting points of final compounds (**7b-f**) was affected by their complex thermal behaviour; consequently, melting points are not reported here. ^{1}H and ^{13}C NMR spectra were obtained on a Bruker Avance 300, at 300 and 75 MHz, respectively, or on a Bruker AC-200, at 200 and 50 MHz, respectively; δ in ppm rel. to $SiMe_4$ as the internal standard; coupling constants *J* in Hz. ^{13}C NMR spectra were fully decoupled. The following abbreviations are used: s: singlet, d: doublet, dd: doublet doublet, t: triplet, qt: quartet, m: multiplet, br: broad, Im: imidazole ring. Mass spectra were recorded on a Finnigan-Mat TSQ-700. Flash chromatography (FC) was performed on BDH silica gel (particle size 40-63 μm). When not otherwise specified, anhydrous magnesium sulphate ($MgSO_4$) was used as drying agent for organic phases. Analysis (C, H, N) of the target compounds was performed by Service de Microanalyse, Université de Genève, Genève (CH), and the results were within ± 0.4% of theoretical values. Derivatives **7a** [21], **3c** [29], **11** [30], and **12** [31] were synthesised by the methods reported. HNE (4-hydroxy-*trans*-2,3-nonenal) was prepared by acid treatment (1mM HCl) of HNE-DMA (4-hydroxy-*trans*-2,3-nonenal-dimethylacetal; Sigma).

4.2. Chemistry

*4.2.1. General procedure for the synthesis of derivatives **7b-f***

To a stirred solution of Fmoc-His-(Trt)-OH (**2**) (2.5 g; 4 mmol) in dry DMF (40 mL), DIPEA (1.03 mL; 6 mmol), HBTU (2.29 g; 6 mmol) and HOBt (0.08 g; 0.6 mmol) were added. After 10 min, the appropriate amine **3b-f** (6 mmol) was added; the reaction mixture was stirred at RT until TLC evidenced complete consumption of starting material (1-18 h). The solvent was removed under reduced pressure (oil pump) and the residue taken up with CH_2Cl_2 (40 mL) and washed with water (3 x 30 mL), brine (30 mL), then dried and evaporated under reduced pressure. The residual oil was purified by flash chromatography, eluting with CH_2Cl_2/MeOH 9.9/0.1 to 9.5/0.5 to afford the desired intermediate **4b-f** (57-94%). To a stirred solution of the resulting intermediate (2.59 mmol) in dry DMF (23 mL), piperidine (1.15 mL; 11.6 mmol) was added and the reaction mixture stirred at RT for 1 h. The solvent was evaporated under reduced pressure and the solid residue was taken up with CH_2Cl_2 (30 mL) and washed with water (3 x 30 mL) and brine (30 mL). The organic phase was dried (Na_2SO_4) and the crude product was purified by flash chromatography, eluting with CH_2Cl_2/MeOH 9.8/0.2 to 8/2 to yield the desired intermediates **5b-f** (74-100%). To a stirred solution of the free amines **5b-f** (1.75 mmol) and Boc-β-Ala-OH (0.35 g; 1.83 mmol) in dry CH_2Cl_2 (30 mL) kept at 0 °C, DCC (0.36 g; 1.75 mmol) was added; the ice bath was removed and the reaction was stirred at RT for 2-18 h. The reaction mixture was cooled to 0 °C. The precipitate was filtered and washed with cold (0 °C) CH_2Cl_2. The liquid phase was washed with water (3 x 30 mL), brine (30 mL), then dried and evaporated under reduced pressure to leave a white solid. The crude material was purified by flash chromatography, eluting with CH_2Cl_2/MeOH 9.8/0.2 to 9.5/0.5 to give the desired derivatives **6b-f** (59-91%) as white foams. The resulting products were dissolved in CH_2Cl_2 (21 mL), treated with CF_3COOH (2.1 mL) and stirred at RT for 20 h. The solvent was evaporated under reduced pressure and the semisolid residue was treated with water (30 mL). The precipitate formed was filtered off through a sintered glass funnel, the water phase was washed with CH_2Cl_2 (2 x 20 mL), then with EtOAc (2 x 20 mL) and evaporated to afford the final products **7b-f**.

*4.2.1.1. β-alanyl-N-[4-(propyloxy)benzyl]-L-histidinamide ditrifluoroacetate (**7b**)*

The product was recrystallized twice from dry MeOH/Et_2O and freeze-dried to yield **7b** as a white foam (67%). ^{1}H-NMR (CD_3OD): δ, 8.71 (s, 1H, ImH_2); 7.24 (s, 1H, ImH_5); 7.13 (d, 2H, *J*=8.4 Hz, Ar$H_{2',6'}$); 6.84 (d, 2H, *J*=8.4 Hz, Ar$H_{3',5'}$); 4.70 (m, 1H, C*H*); 4.30-4.23 (m, 2H, NHCH_2); 3.90 (t, 2H, *J*=6.3 Hz, OCH_2); 3.22-3.08 (m, 4H, ImCH_2, C$H_2NH_3^+$); 2.68-2.62 (m, 2H, COCH_2);

1.80-1.73 (m, 2H, $CH_2CH_2CH_3$); 1.03 (t, 3H, *J*=7.2 Hz, CH_3). ^{13}C-NMR (CD_3OD): δ, 172.4; 171.9; 160; 135; 131.5; 131.2; 130; 118.4; 115.5; 70.6; 53.8; 43.7; 36.8; 32.7; 28.3; 23.7; 10.8. Anal.Calc. for 14 $C_{19}H_{27}N_5O_3$ • 2 CF_3COOH • H_2O, C% 44.59, H% 5.04, N% 11.30. Found: C% 44.60, H% 4.98, N% 11.42.

*4.2.1.2. β-alanyl-N-[3-(nitrooxy)propyl]-L-histidinamide ditrifluoroacetate (**7c**)*
The product was recrystallized from dry MeOH/Et_2O and freeze-dried to yield **7c** as a white foam (89%). ^{1}H-NMR (CD_3OD): δ, 8.81 (s, 1H, ImH_2); 7.35 (s, 1H, ImH_5); 4.64 (m, 1H, C*H*); 4.48 (t, 2H, J = 6.3 Hz, CH_2ONO_2); 3.31-3.10 (m, 6H, ImCH_2, $CH_2NH_3^+$, CH_2NH); 2.68-2.65 (m, 2H, $COCH_2$); 1.92-1.88 (m, 2H, $CH_2CH_2CH_2$). ^{13}C-NMR (CD_3OD): δ, 172.44; 172.41; 135.1; 131.2; 118.4; 72.3; 53.9; 37.1; 36.8; 32.7; 28.0; 27.8. Anal. Calc. for: $C_{12}H_{20}N_6O_5$ • 2 CF_3COOH • H_2O, C% 33.46, H% 4.21, N% 14.63; Found C% 33.83, H% 4.14, N% 14.40.

*4.2.1.3. β-alanyl-N-[(2S)-2,3-bis(nitrooxy)propyl]-L-histidinamide ditrifluoroacetate (**7d**)*
The product was recrystallized twice from dry MeOH/Et_2O and freeze-dried to yield **7d** as a white foam (70%). ^{1}H-NMR (CD_3OD): δ, 8.73 (s, 1H, ImH_2); 7.33 (s, 1H, ImH_5); 5.45 (m, 1H, $CHONO_2$); 4.88-4.58 (m, 3H, C*H*NH, CH_2ONO_2); 3.61-3.41 (m, 2H, $NHCH_2$); 3.30-3.06 (m, 4H, ImCH_2, $CH_2NH_3^+$); 2.86-2.73 (m, 2H, $COCH_2$). ^{13}C-NMR (CD_3OD): δ, 173.1; 172.5; 133.5; 131.2; 118.4; 79.2; 71.2; 54; 39.1; 36.8; 32.6; 27.8. Anal. Calc. for: $C_{12}H_{19}N_7O_8$ • 2 CF_3COOH C% 31.13, H% 3.43, N% 15.,88. Found: C% 31.02, H% 3.61, N% 15.94.

*4.2.1.4. β-alanyl-N-[(2R)-2,3-bis(nitrooxy)propyl]-L-histidinamide ditrifluoroacetate (**7e**)*
The product was recrystallized twice from dry MeOH/Et_2O and freeze-dried to yield **7e** as a white foam (63%). ^{1}H-NMR (CD_3OD): δ, 8.73 (s, 1H, ImH_2); 7.34 (s, 1H, ImH_5); 5.52-5.47 (m, 1H, $CHONO_2$); 4.91-4.86 (m, 1H, C*H*NH); 4.68-4.59 (m, 2H, CH_2ONO_2); 3.74-3.68 (m, 2H, $NHCH_2$); 3.31-3.07 (m, 4H, ImCH_2, $CH_2NH_3^+$); 2.7-2.64 (m, 2H, $COCH_2$). ^{13}C-NMR (CD_3OD): δ, 173.1; 172.6; 135.2; 131.2; 118.4; 79.2; 71.3; 54; 39.2; 36.9; 32.6; 27.8. Anal. Calc. for $C_{12}H_{19}N_7O_8$ • 2 CF_3COOH C% 31.13, H% 3.43, N% 15.88. Found: C% 30.91, H% 3.61, N% 15.97.

*4.2.1.5. β-alanyl-N-{4-[3-(nitrooxy)propyloxy]benzyl}-L-histidinamide ditrifluoroacetate (**7f**)*
The product was recrystallized twice from dry MeOH/Et_2O and freeze-dried to yield **7f** as a white foam (42%). ^{1}H-NMR (CD_3OD): δ, 8.64 (s, 1H, ImH_2); 7.23 (s, 1H, ImH_5); 7.16 (d, 2H, J=8.4 Hz, Ar$H_{2',6'}$); 6.87 (d, 2H, J=8.4 Hz, Ar$H_{3',5'}$); 4.73-4.65 (m, 3H, C*H*, CH_2ONO_2); 4.35-4.23 (m, 2H, $NHCH_2$); 4.06 (t, 2H, J=6 Hz, OCH_2); 3.27-3.05 (m, 4H, ImCH_2, $CH_2NH_3^+$); 2.72-2.60 (m, 2H, $COCH_2$); 2.22-2.14 (m, 2H, $CH_2CH_2CH_2$). ^{13}C-NMR (CD_3OD): δ, 172.3; 172; 159.4; 135.2; 132; 131.6; 130.1; 118.3; 115.6; 71.6; 65.2; 54; 43.7; 36.9; 32.7; 28.6; 28.1. Anal.Calc. for $C_{19}H_{26}N_6O_6$ • 2 CF_3COOH • 2 H_2O, C% 39.55, H% 4.62, N% 12.03. Found: C% 39.19, H% 4.27, N% 12.08.

*4.2.1.6. 4-propoxybenzenemethanamine (**3b**).*
In a flame-dried flask, NaH 60 % in mineral oil (0.80 g; 20.1 mmol) was suspended in dry DMF (20 mL), then *p*-hydroxybenzonitrile (**8**) (2.00 g; 16.8 mmol) was added portionwise and the mixture was stirred for 1 h at RT. After this time, a solution of bromopropane (4.13 g; 33.6 mmol) in dry DMF (10 mL) was added and the reaction stirred for a further 3 h. The mixture was diluted with CH_2Cl_2 (150 mL), washed with water (3 x 100 mL), dried (Na_2SO_4) and evaporated to afford the desired alkylated intermediate, which was dissolved in dry Et_2O (40 mL) and added dropwise

during 30 min to a stirred suspension of $LiAlH_4$ (0.95 g; 25.1mmol) in dry Et_2O (60 mL). When addition was complete, the mixture was refluxed for 30 min, then cooled (0 °C) and cautiously treated with water (10 mL) and CH_2Cl_2 (80 mL), the precipitate formed was filtered through a sintered funnel and the resulting mixture was washed with brine (3 x 40 mL), dried, and evaporated to afford **3b** (2.65 g; 87 %) as a pale yellow oil. The product was used immediately in the next step without further purification.

*4.2.1.7. (2S) 2,3 (dinitrooxy)propan-1-ammonium nitrate (**3d**)*
In a flame-dried flask equipped with a $CaCl_2$ guard tube and an air condenser, (R)-3-amino-1,2-propandiol (1.17 g; 12.8 mmol) was suspended in dry CH_2Cl_2 (34 mL) and kept at 0 °C. Fuming HNO_3 (d= 1.52 g/mL) (3.30 mL) was added cautiously and the mixture stirred vigorously at 0 °C for 2.5 h. Acetic anhydride was slowly added and after 1 h the precipitate was filtered through a sintered glass funnel, collected and dried over P_2O_5, KOH overnight, to afford 2.65 g (85 %) of an off-white solid. The product was recrystallized from iPrOH to obtain a white solid. ^{1}H-NMR (DMSO-d_6): δ, 8.15 (s, br 3H, NH_3^+); 5.68-5.61 (m, 1H, C*H*ONO_2); 4.98 (dd, 2H, J_{gem} = 12.9 Hz; J_{vic} = 3.3 Hz, CH*H*ONO_2); 4.79 (dd, 2H, J_{gem} = 12.9; J_{vic} = 5.4 Hz, C*H*$HONO_2$); 3.38 (dd, 2H, J_{gem} = 14.1; J_{vic} = 3.3 Hz, C*H*HNH_3^+); 3.21 (dd, 2H, J_{gem} = 14.1; J_{vic} = 9.3 Hz, CH*H*NH_3^+). ^{13}C-NMR (DMSO-d_6): δ, 76.4; 70; 37.3, spectral data are in agreement with those of an authentic sample [56]

*4.2.1.8. (2R) 2,3 (dinitrooxy)propan-1-ammonium nitrate (**3e**)*
In a flame-dried flask equipped with a $CaCl_2$ guard tube and an air condenser, kept at 0 °C, dry CH_2Cl_2 (34 mL) and fuming HNO_3 (d= 1.52) (3.30 mL) were mixed cautiously; to this mixture, powdered (R)-3-amino-1,2-propandiol (1.2 g; 13.2 mmol) was added portionwise. The mixture was stirred vigorously at 0 °C for 2 h, then acetic anhydride (3.0 mL; 31.8 mmol) was added and the reaction stirred at 0 °C for a further 45 min The resulting precipitate was filtered through a sintered glass funnel, collected and dried over P_2O_5, KOH overnight, to afford 2.60 g (81 %) of an off-white solid. The product was recrystallized from iPrOH to obtain a white solid. ^{1}H-NMR (DMSO-d_6): δ, 8.16 (s, br 3H, NH_3^+); 5.67-5.62 (m, 1H, C*H*ONO_2); 4.98 (dd, 2H, J_{gem} = 12.9 Hz; J_{vic} = 3.3 Hz, CH*H*ONO_2); 4.79 (dd, 2H, J_{gem} = 12.9; J_{vic} = 5.4 Hz, C*H*$HONO_2$); 3.39-3.33 (m, 2H, C*H*HNH_3^+); 3.21 (dd, 2H, J_{gem} = 14.1; J_{vic} = 9.3 Hz, CH*H*NH_3^+). ^{13}C-NMR (DMSO-d_6): δ, 76.4; 70; 37.3, spectral data are in agreement with those of an authentic sample [57].

*4.2.1.9. 3-[4-(aminomethyl)phenoxy]propyl nitrate (**3f**)*
To a stirred solution of **12** (1.7 g; 5.84 mmol) in dry THF (40 mL) potassium *tert*-butoxide was added, and after 15 min **11** (1.37 g; 6.13 mmol) in dry THF (15 mL) was slowly added. The reaction mixture was stirred at 60 °C for 3 h, cooled and cautiously treated with water (30 mL). The aqueous layer was extracted with CH_2Cl_2 (3 x 30 mL), dried ($MgSO_4$) and evaporated under reduced pressure to afford the expected intermediate as a yellow oil. This oil was dissolved in CH_2Cl_2 (60 mL) and CF_3COOH (4.25 mL) and stirred for 2 h. The solvent was evaporated and the residue taken up with 5 % aqueous $NaHCO_3$, extracted with CH_2Cl_2 (3 x 20 mL) and dried (Na_2SO_4) to leave a orange coloured oil which was purified by flash chromatography, eluting with CH_2Cl_2/MeOH 9.9/0.1 gradient to CH_2Cl_2/MeOH 8/2 to afford the title product in quantitative yield as colourless oil. ^{1}H-NMR ($CDCl_3$): δ, 7.23 (d, 2H, J=8.5 Hz, 2 Ar$H_{2',6'}$); 6.84 (d, 2H, J=8.5 Hz, 2 Ar$H_{3',5'}$); 4.66 (t, 2H, J=6.3 Hz, CH_2ONO_2); 4.04 (t, 2H, J=5.8, OCH_2); 3.79 (m, 2H, CH_2NH_2); 2.24-2.15 (m, 4H, CH_2; NH_2). ^{13}C-NMR ($CDCl_3$): δ, 157.5; 135.2; 128.5; 114.5; 70; 63.6; 45.8; 27. MS CI (isobutane) (m/z): 227 [MH^+].

4.3. Determination of dissociation constants and lipophilicity descriptor

The ionisation constants of the compounds were determined by potentiometric titration with the GLpKa apparatus (Sirius Analytical Instruments Ltd, Forest Row, East Sussex, UK). Ionisation constants of carnosine **1** and compounds **7a-f** were obtained by aqueous titration, with at least four separate titrations for each compound: different aqueous solutions (ionic strength adjusted to 0.15 M with KCl) of the compounds (20 mL, about 1 mM) were initially acidified to pH 1.8 with 0.5 N HCl; the solutions were then titrated with standardized 0.5 N KOH to pH 12.2. Calculated partition coefficients (clog $D_{7.4}$) were obtained from CLOGP (CLOGP for windows, version 4.0, BioByte Corp. Claremont, CA, USA) according to the equation: clog $D_{7.4}$ = CLOGP - log $[1+10^{(pKa2-pH)}+10^{(pKa2-pKa1-2pH)}]$.

The apparent partition coefficients log $D_{7.4}$ were obtained by the shake-flask procedure at pH 7.4 (phosphate buffer solutions with ionic strength adjusted to 0.15 M with KCl); n-octanol was added to the buffers and the two phases were mutually saturated by shaking for 4 h. The compounds were solubilised in the buffered aqueous phase at a concentration of about 0.1 mM and an appropriate amount of n-octanol was added. The two phases were shaken for about 20 min, by which time the partitioning equilibrium of solutes was reached, and then centrifuged (10,000 rpm,10 min). The concentration of solute in the aqueous phase was measured by UV spectrophotometry(UV-2501PC, Shimadzu) at 230 nm. For each compound, at least 6 log *D* values were measured.

4.4. Copper Complexes

Complex formation, between copper(II) and carnosine (**1**) and derivatives **7a**-**f**, was investigated by means of the classical pH-metric technique with the GLpKa apparatus. For each compound, at least three separate titrations were performed: different aqueous solutions of the compounds and of $CuCl_2$ equimolar (1 mM) were initially acidified to pH 1.8 with 0.5 N HCl; the solutions were then titrated with standardized 0.5 N KOH to pH 12.2. The measurements were made under nitrogen at 25.0 ± 0.1 °C and ionic strength adjusted to 0.15 M (KCl). Elaboration of experimental pH-metric data, to calculate the values of formation constants, was done using the BSTAC software [58].

4.5. Stability in human serum

A solution of each compound (10 mM) in water was added to human serum (Sigma) preheated to 37 °C; the final concentration of the compound was 0.5 mM. The solutions were incubated at 37 ± 0.5 °C and, at appropriate time intervals, 500 μL of reaction mixture were withdrawn and added to 500 μL of acetonitrile containing 0.1% trifluoroacetic acid, in order to deproteinize the serum. The sample was sonicated, vortexed and then centrifuged for 10 min at 2150 g. The clear supernatant was filtered through 0.45 μm PTFE filters (Alltech, Deerfield, IL, USA) and analysed by RP-HPLC. HPLC analyses were performed with a HP 1100 chromatograph system (Agilent Technologies, Palo Alto, CA, USA) equipped with a quaternary pump (model G1311A), membrane degasser (G1379A), diode-array detector (DAD) (model G1315B) integrated in the HP1100 system. Data analysis was done using a HP ChemStation system (Agilent Technologies, Palo Alto, CA, USA). The analytical column was a Purospher C18-endcapped (250 × 4.6 mm, 5 μm particle size) (Merck Darmstadt, Germany). The mobile phase consisting of methanol/20 mM CH_3COONa pH 4.5 - 5 mM SDS (80/20 to 60/40 in accordance with the polarity of the compound) and the flow-rate was 0.7 mL/min. The injection volume was 20 μL (Rheodyne, Cotati, CA). The column effluent was monitored at 210 and 223 nm, referenced against a 360 nm wavelength.

4.6. Biological activity

4.6.1. LDL isolation and oxidation

Human plasma from healthy donors was provided by the Blood Bank (A.O. San Giovanni Battista Turin) and fortified with 0.1% EDTA. The LDL fraction was isolated by ultracentrifugation through NaCl discontinuous gradients, and collected as the fraction floating at a density of 1.019-1.063 g/mL. The lag phase (t_{lag}) and propagation rate (R) were determined as described elsewhere [59]. EDTA was removed by rapid filtration through disposable desalting columns Econo-Pac 10 DG (Bio-Rad). Filtered LDL aliquots were diluted with PBS (10 mM phosphate buffer, pH 7.4) to give a final concentration of 50 μg LDL protein/mL, and transferred to a 1-cm cuvette, either with 50 μL of water alone, or with 50 μL of the test compound solution in water at a final concentration of 100 μM. Formation of conjugated dienes was measured spectrophotometrically in a Varian Cary 50 Bio spectrophotometer, equipped with a thermostatic control (37 °C) and an automatically exchangeable multi-position cuvette holder, operating at 234 nm. Oxidation was initiated by adding to the LDL a suspension of $CuSO_4$ at a final concentration of 2.5 μM.

4.6.2. HNE scavenging studies

HNE (final concentration 50 μM in 1 mM phosphate buffer, pH 7.4) was incubated with a solution of compounds **7a-f**, or with carnosine (**1**) (final concentration 1 mM in 1 mM phosphate buffer, pH 7.4) for different periods (up to 24 h) at 37 °C. Samples for each different incubation time were analyzed directly by HPLC to measure HNE consumption, as described elsewhere [7]. HNE was determined by reverse-phase HPLC, using a HP 1100 chromatograph system (Agilent Technologies, Palo Alto, CA, USA) previously described. Reaction mixture (20 μL) was eluted on a Agilent Zorbax Eclipse XDB-C18 column (150 x 4.6 mm; particle size 5 μm). The mobile phase was 60% A (water/acetonitrile/formic acid; 9:1:0.01, v/v/v) and 40% B (water/acetonitrile; 1:9, v/v) delivered at a flow-rate of 1 mL/min. The column effluent was monitored at 223 nm.

4.6.3. Vasodilator activity assay.

Thoracic aortas were isolated from male Wistar rats weighing 180-200 g. The endothelium was removed and the vessels were cut helically: three strips were obtained from each aorta. The strips were mounted in organ baths containing 30 mL of Krebs-bicarbonate buffer of the following composition (mM): NaCl 111.2, KCl 5.0, $CaCl_2$ 2.5, $MgSO_4$ 1.2, KH_2PO_4 1.0, $NaHCO_3$ 12, glucose 11.1 maintained at 37 °C and continuously gassed with 95% O_2-5% CO_2 (pH=7.4). The aortic strips were allowed to equilibrate for 90 min and then contracted with 1 μM L-phenylephrine. When the response to the agonist reached a plateau, cumulative concentration–response curves were determined. The effect of 1 μM ODQ was evaluated in a separate series of experiments, in which the inhibitor of sGC was added 5 min before contraction. EC_{50} values are the mean of at least 5 determinations. Responses were recorded by an isometric transducer connected to the MacLab System PowerLab.

4.7. In vivo experimental protocols

4.7.1. Animals and surgery.

Male Wistar rats (Harlan-Italy; Udine, Italy) weighing 210 to 230 g were housed in a controlled environment at 25±2 °C with alternating 12-h light and dark cycles. They were provided with a Piccioni pellet diet (n.48, Gessate Milanese, Italy) and water *ad libitum*. All rats were acclimatized in our animal facility for at least 1 week prior to experiments, and stressful stimuli were avoided.

Animal care was in compliance with Italian regulations on the protection of animals used for experimental and other scientific purposes (D.M. 116/92) as well as with the Guide for the Care

and Use of Laboratory Animals, as adopted and promulgated by the U.S. National Institutes of Health. The experimental protocol, approved by the Turin University Ethics Committee, was performed as described elsewhere [48]. Briefly, rats were anaesthetised with i.p. injection (30 mg/kg) of Zoletil 100 (mixture of tiletamine and zolazepam, Laboratoires Virbac, France), which was supplemented as needed. Anaesthetised rats were placed onto a thermostatically controlled heating pad, a rectal temperature probe was inserted and body temperature was monitored and maintained at 37 °C. Both common carotid arteries were exposed over a midline incision and a dissection was made between the sternocleidomastoid and the sternohyoid muscles, parallel to the trachea. Each carotid artery was freed from its adventitial sheath and vagus nerve, which was carefully separated and maintained. Ischemia was achieved by clamping the bilateral common carotid arteries for 30 min, using non-traumatic artery clamps (Micro Bulldog Clamps, Harvard Apparatus Ltd., Kent, U.K.).
During ischemia, the animals were monitored for body temperature, respiration pattern, loss of righting reflex, unresponsiveness, corneal reflexes, and fixed and dilated pupils. Recirculation of blood flow was established by releasing the clips, and restoration of blood flow in the carotid arteries was confirmed by careful observation. Reperfusion was allowed for 24 h. Post-surgery, the animals were kept for at least 3 h in a 37 °C incubator to ensure that postoperative recovery was satisfactory. Thereafter, they were group-housed under temperature- and light-controlled conditions, with food and water *ad libitum*. At the end of the reperfusion period, the rats were anaesthetised and killed by decapitation, after aortic exsanguination; the forebrain was rapidly dissected at 0 °C. Sham-operated rats underwent identical surgical procedures, except that no artery clamps were applied.

4.7.2. Drug treatments.
Animals were randomly allocated into different groups (n = 5 per group): Sham (the common carotid arteries were exposed but not occluded); I/R group; carnosine group (the drug was administered at 1 g/kg); compound **7e** group (the drug was administered at 500 mg/kg) and des-NO analogue **7a** group (the drug was administered at 500 mg/kg). All compounds were prepared in 5% DMSO and injected i.v., at the beginning of reperfusion and again after 6 h. For all experiments, concentrations of drugs were calculated such that all animals received equal volumes of DMSO.
The dose of carnosine used was based on that previously shown to attenuate injury in animal models of cerebral I/R injury [49].

4.7.3 Determination of infarct volume.
After 24 h of reperfusion, the rats were killed with an overdose of Zoletil 100 (mixture of tiletamine and zolazepam) and decapitated. The rats' brains were immediately removed and placed in ice-cold saline for 5 min. Each brain was then placed in a brain matrix and coronal sections were cut into 2- mm slices. Brain slices were immediately immersed in 2% 2,3,5-triphenyltetrazolium chloride monohydrate (TTC) solution (in saline) at 37 °C for 30 min, followed by 4% paraformaldehyde solution. The infarct area and hemisphere area of each section were traced and quantitated by a computerized image analysis system (Inquiry; Loats, Westminster, MD, U.S.A.) and the infarct area was expressed as a percentage of the whole brain area.

4.7.4. Determination of serum tumour necrosis factor (TNF)-α concentration.

TNF-α serum concentrations were measured using commercial enzyme-linked immunosorbent assay (ELISA) kits (Cayman Chemical, Ann Arbor, MI), following the protocol provided by the manufacturer; results are expressed as pg/mL.

4.7.5. Statistical analysis.

All values in both the text and figures are expressed as means ± standard error of the mean (S.E.M.) for n observations. One-way analysis of variance with Dunnett's post test was performed using GraphPad Prism version 4.02 for Windows (GraphPad Software, San Diego, California, USA) and p values below 0.05 were considered to be significant.

Acknowledgments

This work was supported by Regione Piemonte, "Progetto di Ricerca Sanitaria Finalizzata", Bando Regionale 2009.

References and notes

[1] A. A. Boldyrev Carnosine and Oxidative Stress in Cells and Tissues. Nova Science Publishers, Inc.: New York, 2006.
[2] a) J. F. Lenney, R. P. George, A. M. Weiss, C. M. Kucera, P. W. Chan, G. S. Rinzier, Clin. Chim. Acta 123 (1982) 221–231. b) A.Pegova, H. Abe, A. Boldyrev, Comp. Biochem. Physiol. B-Biochemistry & Molecular Biology 127 (2000) 443-446.
[3] A. R. Hipkiss in Advances in Food and Nutrition Research, S. Taylor ed., Academic Press 2010, pp. 87-154.
[4] R. Kohen, Y. Yamamoto, K. C. Cundy, B. N. Ames, Proc. Natl. Acad. Sci. U. S. A. 85 (1988) 3175-3179.
[5] A. R. Hipkiss, J. Alzheimer's Dis. 11 (2007) 229–240, and references therein.
[6] A. Guiotto, A. Calderan, P. Ruzza, G. Borin, Curr. Med. Chem. 12 (2005) 2293-2315.
[7] G. Aldini, M. Carini, G. Beretta, S. Bradamante, R. Maffei Facino, Biochem. Biophys. Res. Commun. 298 (2002) 699–706.
[8] G. Aldini, R. Maffei Facino, G. Beretta, M. Carini, Biofactors 24 (2005) 77-87, and references therein.
[9] A. R. Hipkiss, J. Michaelis, P. Syrris, FEBS Lett. 371 (1995) 81–85.
[10] L. Hobart, I. Seibel, G. S. Yeargans, N. W. Seidler, Life Sci. 75 (2004) 1379–1389.
[11] M. Takeuchi, S. Yamagishi, Curr. Pharm. Des. 14 (2008) 973-978.
[12] S. Bennett, M. M. Grant, S. Aldred, J. Alzheimer's Dis. 17 (2009) 245-257.
[13] F. Bellia, G. Vecchio, S. Cuzzocrea, V. Calabrese, E. Rizzarelli, Mol. Aspects of Med. 32 (2011) 258-266.
[14] C. Corona, V. Frazzini, E. Silvestri, R. Lattanzio, R. La Sorda, M. Piantelli, L. M. T. Canzoniero, D. Ciavardelli, E. Rizzarelli, S. L. Sensi PloS ONE 6(3) 2011, e17971.
[15] F. Bellia, G. Vecchio, E. Rizzarelli, Amino Acids EPub ahead of print, DOI 10.1007/s00726-011-1178-6.
[16] G. Vistoli, M. Carini, G. Aldini, Amino Acids, EPub ahed of print, DOI 10.1007/s00726-012- 1224-z.
[17] G. Vistoli, M. Orioli, A. Pedretti, L. Regazzoni, R. Canevotti, G. Negrisoli, M. Carini, G. Aldini, ChemMedChem 4 (2009) 967-975.
[18] R. Di Paola, D. Impellizzeri, A. Trovato Salinaro, E. Mazzon, F. Bellia, M. Cavallaro, C. Cornelius, G. Vecchio, V. Calabrese, E. Rizzarelli, S. Cuzzocrea, Biochem. Pharmacol. 82 (2011) 1478-1489.

[19] M. Orioli, G. Vistoli, L. Regazzoni, A. Lapolla, G. Rossoni, R. Canevotti, L. Gamberoni, M. Previtali, M. Carini, G. Aldini, ChemMedChem 6 (2011) 1269-1282.
[20] V. Lanza, F. Bellia, R. D'Agata, G. Grasso, E. Rizzarelli, G. Vecchio J. Inorg. Biochem. 105 (2011) 181-188.
[21] M. Bertinaria, B. Rolando, M. Giorgis, G. Montanaro, S. Guglielmo, M. F. Buonsanti, V. Carabelli, D. Gavello, P. G. Daniele, R. Fruttero, A. Gasco, J. Med. Chem. 54 (2011) 611-621, and references therein.
[22] C. Napoli, L. J. Ignarro, Arch. Pharm. Res. 32 (2009) 1103-1108.
[23] C. Humpel, Exp. Gerontol. 46 (2011) 225-232.
[24] J. C. de la Torre, G. B. Stefano, in Biomedical Significance of Nitric Oxide, G. B. Stefano, Ed. Medical Science International: Warsaw-New York, 2003, 213.
[25] V. Calabrese, C. Mancuso, M. Calvani, E. Rizzarelli, D. A. Butterfield, A. M. Giuffrida Stella, Nat. Rev. Neurosci. 8 (2007) 766-775.
[26] V. Calabrese, C. Cornelius, E. Rizzarelli, J. B. Owen, A. T. Dinkova-Kostova, A. D. Butterfield, Antiox. Redox. Signal. 11 (2009) 2717-2740.
[27] M. C. Martinez, R. Andriantsitohaina, Antiox. Redox. Signal. 11 (2009) 669-702.
[28] K. Chegaev, C. Cena, M. Giorgis, B. Rolando, P. Tosco, M. Bertinaria, R. Fruttero, P-A. Carrupt, A. Gasco, J. Med. Chem. 52 (2009) 574-578.
[29] L. B. Romanova, M. E. Ivanova, D. A. Nesterenko, L. T. Eremenko, Russ. Chem. Bull. 43, (1994) 1207-1209.
[30] K. Chegaev, L. Lazzarato, B. Rolando, E. Marini, P. Tosco, C. Cena, R. Fruttero, F. Bertolini, M. Reist, P. A. Carrupt, V. Lucini, F. Fraschini, A. Gasco, J. Pineal Res. 42 (2007) 371-385.
[31] K. S. Chichak, A. J. Peters, S. J. Cantrill, J. Fraser Stoddart, J. Org. Chem. 70 (2005) 7956-7962.
[32] A.A. Boldyrev, S.L. Stvolinsky, T.N. Fedorova, and Z.A. Suslina. Rejuv. Res. 13 (2010) 156- 158.
[33] G. Vistoli, A. Pedretti, M. Cattaneo, G. Aldini, B. Testa, J. Med. Chem. 49 (2006) 3269–3277.
[34] P. G. Daniele, E. Prenesti, V. Zelano, G. Ostacoli, Spectrochim. Acta, Part A 9 (1993) 1299–1306.
[35] E. J. Baran, Biochemistry (Moscow) 75 (2000) 928–937.
[36] M. Kuzuya, K. Yamada, T. Hayashi, C. Funaki, M. Naito, K. Asai, F. Kuzuya, Biochim. Biophys. Acta 123 (1992) 334-341.
[37] R. P. Patel, D. Svistunenko, M. T. Wilson, V.M. Darley-Usmar, Biochem. J. 322 (1997), 425– 433.
[38] O. Ziouzenkova, A. Sevanian, P. M. Abuja, P. Ramos, H. Esterbauer, Free Radical. Biol. Med. 24 (1998) 607-623.
[39] R. Sultana, M. Perluigi, D. A. Butterfield, Antiox. Redox Signal. 8 (2006) 2021-2037.
[40] M. K. Eberhardt, Reactive oxygen metabolites: chemistry and metabolic consequences. CRC Press LLC: 2000; pp 365-378.
[41] A. A. Fouad, M. A. El-Rehany, H. K. Maghraby, Eur. J. Pharmacol. 572 (2007) 61-68.
[42] H. Kurata, T. Fujii, H. Tsutsui, T. Katayama, M. Ohkita, M. Takaoka, N. Tsuruoka, Y. Kiso, Y. Ohno, Y. Fujisawa, T. Shokoji, A. Nishiyama, Y. Abe, Y. Matsumura, J. Pharmacol. Exp. Ther. 319 (2006) 640-647.
[43] C. Pekcetin, M. Kiray, B. U. Ergur, K. Tugyan, H. A. Bagriyanik, G. Erbil, B. Baykara, U. M. Camsari, Acta Biol. Hung. 60 (2009) 137-148.
[44] K. L. Chan, Curr. Med. Chem.: Anti-Inflammatory Anti-Allergy Agents 1 (2002) 1-13.

[45] A. de Mel, F. Murad, A. M. Seifalian, Chem. Rev. 111 (2011) 5742-67.
[46] M. Willmot, L. Gray, C. Gibson, S. Murphy, P. M. W. Bath, Nitric Oxide 12 (2005) 141-149.
[47] P. Zhuang, H. Ji, Y.-H. Zhang, L. Z. Min, Q.-G. Ni, R. You, Clin. Exper. Pharmacol. Physiol. 37 (2010) e121-e127.
[48] a) M. Collino, S. Castiglia, M. Manoni, L. Salsini, J. Chini, E. Masini, R. Fantozzi, Thromb. Haemost. 102 (2009) 837-845. b) M. Collino, M. Aragno, R. Mastrocola, E. Benetti, M. Gallicchio, C. Dianzani, O. Danni, C. Thiemermann, R. Fantozzi, Free Rad. Biol. Med. 41 (2006) 579-589.
[49] J. Min, M.-C. Senut, K. Rajanikant, E. Greenberg, R. Bandagi, D. Zemke, A. Mousa, M. Kassab, M. U. Farooq, R. Gupta, A. Majid, J. Neurosci. Res. 86 (2008) 2984-2991.
[50] Y. Shen, P. He, Y. Fan, J. Zhang, H.Yan, W. Hu, H. Ohtsu, Z. Chen, Free Rad. Biol.Med. 48 (2010) 727-735.
[51] X. Zhang, L. Song, X. Cheng, Y. Yang, B. Luan, L. Jia, F. Xu, Z. Zhang, Eur J Pharmacol 667 (2011) 202-207.
[52] D. Dobrota, T. Fedorova, S.Stvolinsky, E. Babusikova, K. Likaveanova, A. Drgova, A. Strapkova, A. Boldyrev, Neurochem Res 30 (2005) 1283-1288.
[53] A. K. Khama-Murad, A.A. Mokrushin, L.I. Pavlinova, Regulatory Peptides 167 (2011) 65-69.
[54] a) M. Collino, M. Aragno, S. Castiglia, C. Tomasinelli, C. Thiemermann, G. Boccuzzi, R. Fantozzi, Diabetes 58 (2009) 235-242. b) A. Tuttolomondo, R. Di Sciacca, D. Di Raimondo, C. Renda, A.Pinto, G. Licata, Curr. Top. Med. Chem. 9 (2009) 1240-1260.
[55] C. Popa, M. G. Netea, P. L. C. M. van Riel, J. W. M. van der Meer, A. F. H. Stalenhoe, J Lipid Res. 48 (2007) 751-762.
[56] D.S. Garvey, L. G. Letts, R. A. Earl, M. Ezawa, X. Fang, R. D. Gaston, S. P. Khanapure, C-E. Lin, R. R. Ranatunge, C. A. Stevenson, S-J. Wey, US2006/0189603.
[57] D.S. Garvey, R. A. Earl, M. Ezawa, X. Fang,L. R. D. Gaston, S. P. Khanapure, C-E. Lin, R. R. Ranatunge, C. A. Stevenson, S-J. Wey, US2005/030135.
[58] C. De Stefano, P. Mineo, C. Rigano, S. Sammartano, Ann. Chim. (Rome) 83 (1993) 243-277.
[59] Esterbauer, H.; Striegl, G.; Puhl, H.; Rotheneder, M, Free Rad. Res. Comms. 6 (1989) 67-75.

Table 1. Dissociation constants (pK_a), formation constants ($\log \beta_{pqr}$) of copper(II) complexes and logarithm of the ratio between $[Cu^{2+}]_{total}$ and $[Cu^{2+}]_{free}$ for carnosine (**1**) and derivatives **7a-f**.

N.	pK_{a1} [a]	pK_{a2} [a]	$\log\beta_{111}$	$\log\beta_{110}$	$\log\beta_{11-1}$	$\log\beta_{22-2}$	$\log\beta_{22-3}$	$\log\beta_{22-4}$	$\log\beta_{120}$	$\log([Cu^{2+}]_{tot}/[Cu^{2+}]_{free})$ [c]
1 [b]			13.30	8.47	2.44	8.35			14.05	3.81
7a [b]	6.18	9.19	12.22	6.72	1.25	5.40	-3.09	-12.67	13.47	2.93
7b	6.22	9.19	[d]	[d]	[d]	[d]	[d]	[d]	[d]	[d]
7c	6.16	9.19	12.27	6.81	1.22	6.14	-2.73	-12.68	13.49	3.06
7d	6.19	9.21	12.10	6.42	1.21	5.24	-3.52	-13.08	13.29	3.00
7e	6.19	9.23	12.34	7.15	1.39	6.22	-2.47	-12.01	13.28	3.05
7f	6.21	9.16	[d]	[d]	[d]	[d]	[d]	[d]	[d]	[d]

[a] Determined by potentiometric titration with GLpKa apparatus; $n \geq 4$, SD < 0.03; carnosine pK_{a1-3} were respectively 2.60, 6.79, 9.42. [b] ref.[21]. [c] Calculated for $[Cu^{2+}]_{total} = 2.5 \times 10^{-6}$ mol L^{-1} and $[ligand]_{total} = 1 \times 10^{-4}$ mol L^{-1} at pH 7.4. [d] Not determined because of low solubility of compounds in experimental conditions.

Table 2. Lipophilicity, antioxidant activity, HNE-scavenging ability and vasodilator properties of carnosine (**1**) and derivatives **7a-f**.

N.	Lipophilicity	Antioxidant activity		HNE-scavenging ability	Vasodilator properties
	log $D^{7.4a}$	Δt_{lag} (min) ± SEM[b]	R (nmol min^{-1} mg^{-1} LDL prot) ± SEM[b]	HNE % scavenged ± SEM 24 h[c]	EC_{50} ± SEM (μM)[d]
1	nd	67 ± 2	5.8 ± 0.3	88.8 ± 1.6	nd
7a	-2.72	68 ± 2	7.7 ± 0.3	81.0 ± 1.6	nd
7b	-1.15	64 ± 6	9.5 ± 0.5	73.3 ± 1.3	nd
7c	-2.43	90 ± 3	3.9 ± 0.2	75.4 ± 3.5	[e]
7d	-2.33	75 ± 4	5.8 ± 0.1	67.2 ± 4.5	169 ± 30
7e	-2.19	88 ± 3	5.8 ± 0.3	77.6 ± 3.2	70 ± 11
7f	-1.01	70 ± 1	6.3 ± 0.2	74.3 ± 2.7	3.0 ± 0.5

[a] Determined by the shake-flask technique; $n \geq 6$, SD < 0.06. [b] Obtained by $CuSO_4$-induced human LDL oxidation assay in the presence of compounds at 100 μM. *R* values were calculated from ΔA_{234} as a function of time, using ε_{234} = 29500 M^{-1} cm^{-1} for conjugated lipid peroxides. For control LDL samples, *R*= 12.1 ± 0.5 nmol min^{-1} mg^{-1} LDL prot. [c] Determined in phosphate buffer (pH 7.4, 1 mM) at 37 °C; HNE (50 μM), test compound (1 mM). Scavenging % was calculated from the following formula: scavenging (%) = 100 −{[(amount of HNE left after *t* h in the presence of the scavenger) / (amount of HNE left after *t* h in the control)] x 100} [d] The EC_{50} value represents the μM equivalents of test compounds required to relax the precontracted rat aorta strips by 50%. [e] 46 ± 3 % tissue relaxation at the maximum concentration tested (1mM). nd = not determined.

Chart 1

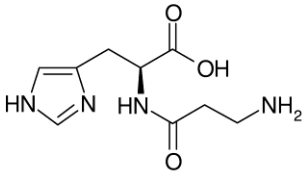

carnosine (1)

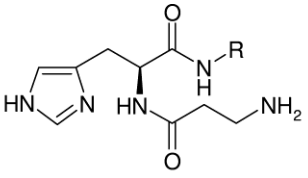

I; R = alkyl or arylalkyl

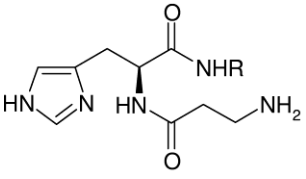

7a-**f**

7a; R = 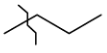

7b; R = 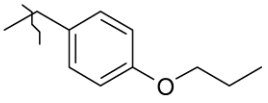

7c; R = 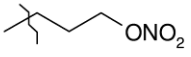

7d; R = 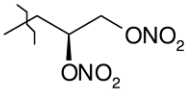

7e; R = 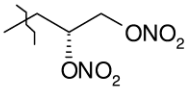

7f; R = 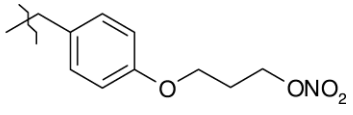

Scheme 1

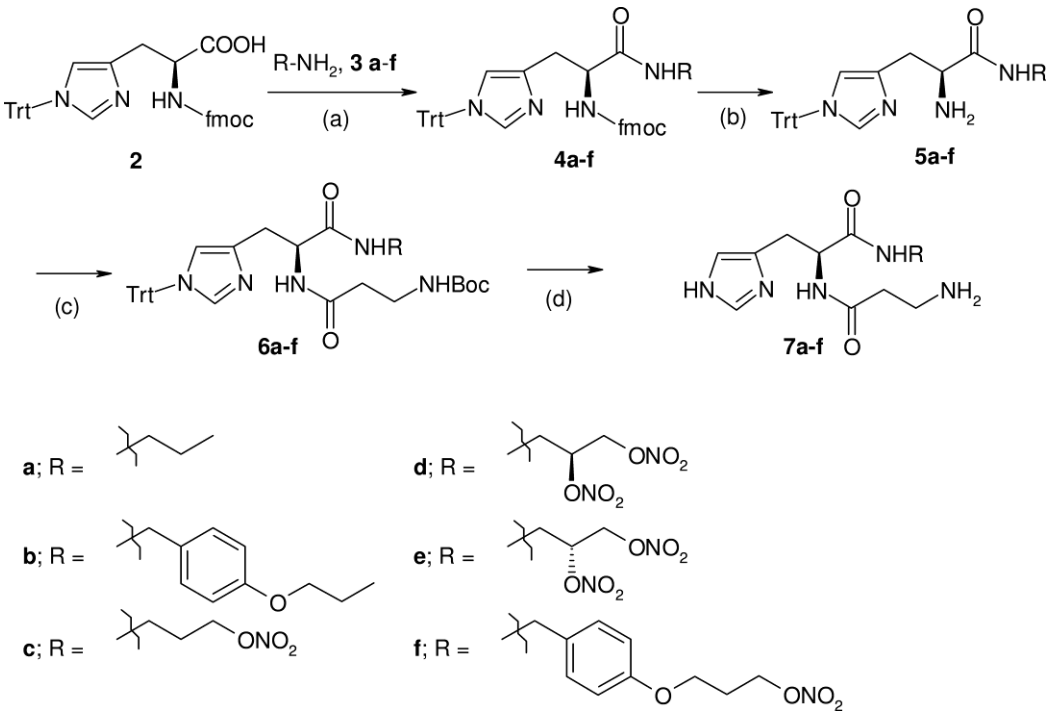

Scheme 1. Preparation of derivatives **7a-f**. Reagents and conditions: (a) DIPEA, HBTU, $HOBt_{cat}$, 10 min RT, then **3a-f** 1-18 h, RT (57-94 %); b) Piperidine , dry DMF, 1 h, RT. (74-100 %); c) Boc-β-Ala(OH), DCC, dry CH_2Cl_2, 0 °C to RT. 2-18 h. (59-91 %); d) CF_3COOH 10 % in CH_2Cl_2, 20 h ,RT (34-89 %).

Scheme 2

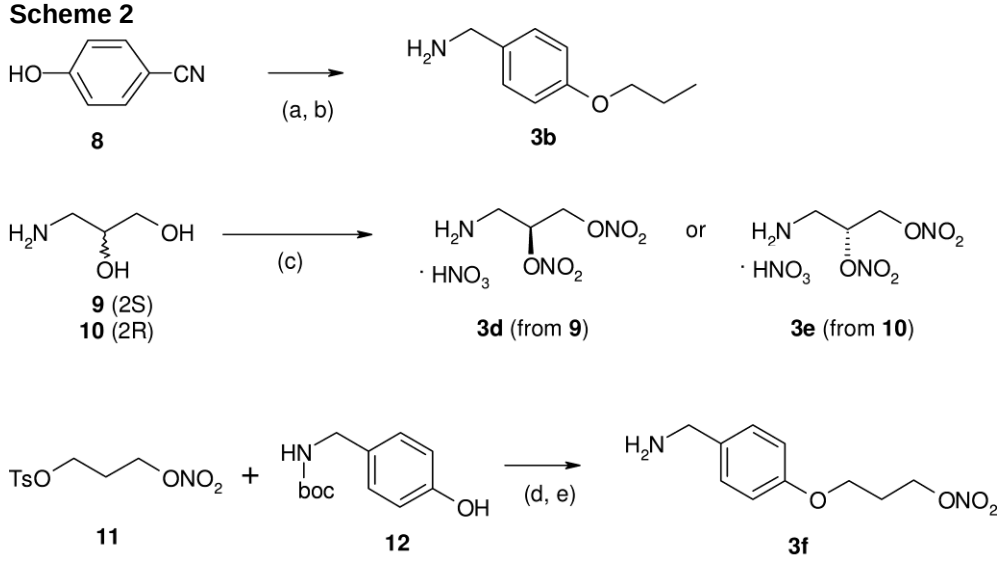

Scheme 2. Preparation of intermediate amines **3b, 3d-f**. Reagents and conditions: (a) NaH, RT, dryDMF, 1h, then 3-Bromopropane, RT, 3 h; (b) $LiAlH_4$, dry Et_2O, RT to reflux, 30 min; (c) fumingHNO_3, 0 °C, dry CH_2Cl_2, 2 h, then Ac_2O, 0 °C, 1 h; (d) *Tert*-BuOK, THF dry, RT, 15 min then reflux 3 h; (e) CF_3COOH 10 % in CH_2Cl_2, 2 h , RT.

Figure 1. a) Relationship between antioxidant activity (expressed as Δt_{lag}) and calculated lipophilicity (clog $D_{7.4oct}$) obtained for carnosine amide derivatives (○) [21] and for new compound**7b** (●). Calculated clog $D_{7.4oct}$ for designed NO-donor analogues **7c-f** (▲) is also reported. b)Relationship between antioxidant activity (expressed as Δt_{lag}) and measured lipophilicity (log$D_{7.4oct}$) obtained for all carnosine amide derivatives: (○) compounds described in [21], (●) new reference compound **7b,** (▲) NO-donor carnosine analogues **7c-f** .

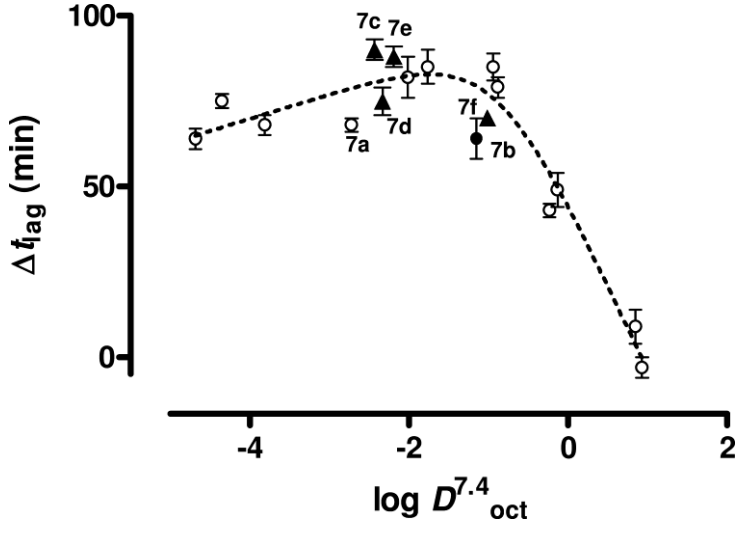

Figure 2. Effects of carnosine derivatives on infarct volume induced by cerebral I/R injury. Effects evoked by the administration of carnosine (**1**) (1 g/kg), compound **7e** (500 mg/kg) or its des-NO analogue **7a** (500 mg/kg) on cerebral infarct volume were evaluated at 24 h reperfusion. Data are means ± S.E.M. of five animals/group. ★ $p < 0.01$ versus I/R.

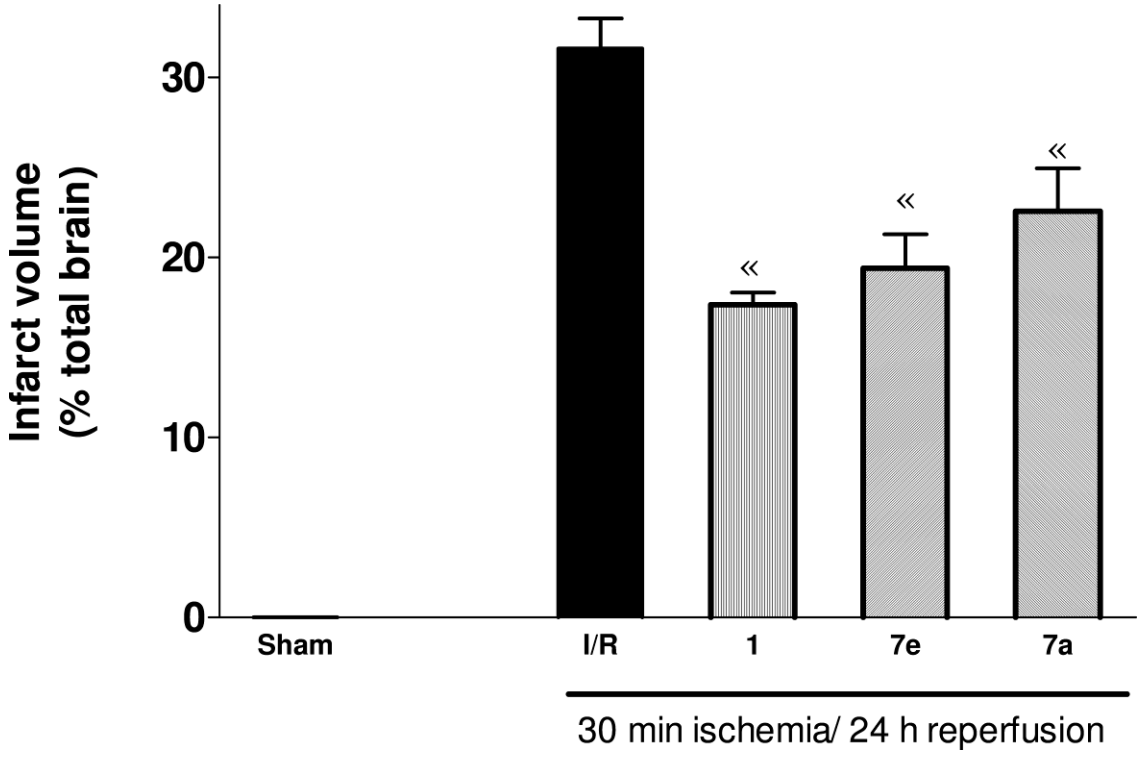

Figure 3. Alterations in serum levels of TNF-α induced by compound **7e**. Rats were subjected to 30min ischemia and 24 h reperfusion (I/R). Carnosine (**1**) (1 g/kg), compound **7e** (500 mg/kg) or its des-NO analogue **7a** (500 mg/kg) were administered during reperfusion. Data are means ± S.E.M. of five animals per group. ● $p < 0.05$ versus **7e.**